  Bull. Chem. Soc. Jpn., 60, 1617—1623 (1987)

ESR and Mass Spectrometric Studies of Methanol Combustion. II. Correlation between Labile and Stable Chemical Species in Methanol-Oxygen-Argon Flame at Low Pressure

Masayuki TANIGUCHI, Toshiharu YOSHIOKA,† and Hiroshi YOSHIDA*
Faculty of Engineering, Hokkaido University, Kita-ku, Sapporo 060
(Received November 11, 1986)

In order to experimentally elucidate the chemical reactions of methanol combustion, the concentration profiles of ten chemical species were determined in stoichiometric CH_3OH–O_2–Ar flat flame at low pressure, 1.11×10^4 Pa. The concentrations of three labile intermediates (H, O, and OH) as well as that of stable O_2 molecules, were measured by means of the probe-sampling-ESR method. The concentrations of six stable species (CH_3OH, CH_2O, CO, CO_2, H_2, and H_2O) were measured using a quadrupole mass spectrometer. The rates of the net chemical formation (or decay) of these species were determined by subtracting the effect of diffusion from their observed concentration profiles, and were examined on the basis of the reaction mechanisms previously proposed for methanol combustion. The experimental results were found to be consistent with the oxidation pathway $CH_3OH\rightarrow CH_2OH\rightarrow CH_2O\rightarrow CHO\rightarrow CO\rightarrow CO_2$. The results also showed that the reaction $CH_2OH+O_2\rightarrow CH_2O+HO_2$ is an important pathway for O_2 consumption.

In order to elucidate complex combustion reactions in flames, it is indispensable to determine the concentration profiles of as many chemical species, both labile and stable, as possible in the flames. However, it is a difficult task to determine the concentration profiles, especially, of the labile intermediates in high temperature flames. We have been using the probe-sampling-electron spin resonance (ESR) technique to detect the labile intermediates (H, O, and OH; the principal carriers of chain reactions of combustion), in free-burning methane and methanol flames.[1,2] Recently, we carried out a combined ESR-mass spectrometric study in order to examine the concentration profiles of nine (labile and stable) chemical species in free-burning methanol-air flames at atmospheric pressure (in the previous study of this series).[3] The study was extended in our work to the CH_3OH–O_2–Ar flames at a low pressure; this allowed us to control more strictly the physical conditions of combustion and to change more freely the equivalence ratio of the premixed gas.

The reaction mechanism of methanol combustion has theoretically been studied over ten years;[4–7] several numerical models concerning combustion reactions, including more than twenty species, have been proposed.[6–8] However, most of the experimental data so far reported[4,5,9–11] have only partially shown chemical features of the combustion, and have not been sufficiently comprehensive for a comparison with theoretical predictions and to substantiate the proposed models. Akrich et al. first determined the concentration profiles of stable chemical species in methanol-air flames at low pressures by means of the gas chromatographic method.[9] Pauwels et al.[10] later studied the concentration profiles of H, O, and OH by means of the ESR method under the same flame conditions as those in the above gas chromatographic study; these gave general support to the numerical model proposed by Westbrook and Dryer.[6] Very recently, Vandooren and Van Tiggelen,[11] and Andersson et al.[4] performed mass spectrometric studies and obtained a comprehensive set of the profiles of stable species and labile intermediates in methanol flames at low pressures. Based on these results, Dove and Warnatz[7] developed a simplified model of methanol combustion. The present ESR-mass spectrometric study complements these previous studies and serves as an experimental basis for obtaining a further insight into chemical reactions during methanol combustion.

Experimental

The burner and sampling system used in the present study is schematically shown in Fig. 1. The burner comprised two concentric stainless-steel tubes: The inner tube was attached with a porous stainless-steel disk (27-mm diameter) at the end which acted as the burner mouth, and the outer tube (58-mm diameter) enclosed the flame at a low pressure and supported a quartz sampling probe. The sampling probe was pretreated with an aqueous HF solution and cleaned with aqueous NaOH and HNO_3 solutions in order to reduce the surface destruction of labile intermediates.[2,10] Sampling of burning gas was made at several positions on the center axis of the flame by sliding the inner tube with respect to the outer one. The burner was cooled by circulating water.

Oxygen, and argon of purity higher than 99.9% were supplied from cylinders through regulated rotermeters. Methanol of reagent grade was continuously injected into preheated gas flow with a microfeeder. The flames of premixed gas, CH_3OH–O_2–Ar, were stabilized in the burner at a low pressure (1.11×10^4 Pa); this was controlled by adjusting the pumping rate.

The ESR and mass spectrometric measurements of burning gas were made with an X-band ESR spectrometer

† Present address: Nihon Furnace Kogyo, Ltd., Tsurumi-ku, Yokohama 230.

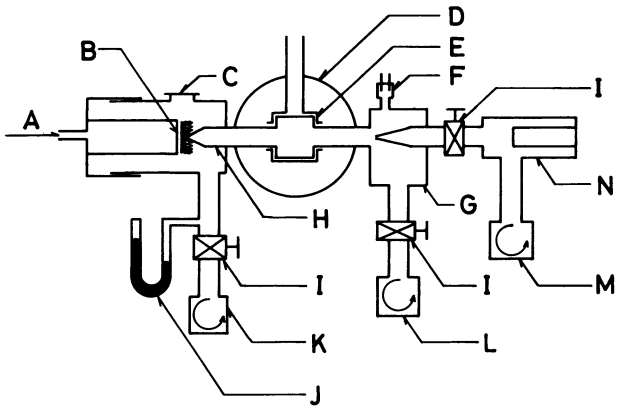

Fig. 1. Schematic drawing of the burner and the sampling system. A) Inlet of premixed gases, B) porous stainless-steel plate, C) viewing window, D) magnet, E) ESR spectrometer, F) vacuum gauge, G) condenser, H) sampling probe, I) vacuum valve, J) Hg manometer, K) primary pumping system (rotary pump), L) secondary pumping system (rotary pump and mechanical booster pump), M) tertiary pumping system (rotary pump and diffusion pump), and N) quadrupole mass spectrometer.

and a quadrupole mass spectrometer (as previously described).[3] About one-tenth of the burning gas was continuously sampled through a tiny hole (about 0.1 mm in diameter) at the tip of the sampling probe; it was subjected to ESR measurements at 13.3 Pa and mass spectroscopic measurements at a total pressure of 10^{-3} Pa. The residence time of the sampled gas in the sampling probe before reaching the ESR cavity was estimated to be about 2 ms. The flame temperature was measured with a SiO_2-coated Pt/Pt-Rh thermocouple.

Analysis of Data

From the apparent local concentration obtained by ESR or mass spectrometric measurements of the i-th species at each position in the flame, the mass flux was calculated as

$$G_i = \frac{X_i M_i}{\bar{M}}\left(1+\frac{V_i}{v}\right), \tag{1}$$

where $\bar{M}$ is the average molecular weight, v the velocity of the flame gas, and X_i, M_i, and V_i the mole fraction, the molecular weight, and the diffusion velocity of the i-th species in the flame gas. By taking the z-axis along the gas flow, the diffusion velocity was calculated as

$$V_i = -\frac{D_{ij}}{X_i}\cdot\frac{dX_i}{dz}, \tag{2}$$

using the binary diffusion coefficients D_{ij} given by

$$D_{ij} = \frac{1.66\times 10^{-3}(1/M_i+1/M_j)^{1/2}T^{1.67}}{P\sigma_{ij}^2(\varepsilon_{ij}/\kappa)^{0.17}} \tag{3}$$

as well as the Lennard-Jones potential parameters (σ_{ij} and ε_{ij}/κ) derived by Westenberg and Fristrom,[12] and Warnatz.[13] In actual calculations, argon was always taken as the j-th species.

The net reaction rate was then calculated as

$$K_i = \frac{\rho v}{M_i}\cdot\frac{dG_i}{dz}, \tag{4}$$

where ρ is the density of the flame gas. This quantity gives the rate of net formation (or consumption) at a particular position in the flame solely due to chemical reactions involving the i-th species, i.e., the net formation rate derived by subtracting the effect of diffusion from the concentration profile observed by ESR or mass spectrometric measurements.

Results and Discussion

Concentration Profiles. ESR spectra due to H, O, OH, and O_2 were observed in the present CH_3OH–O_2–Ar flame. The spectral features were essentially the same as those previously observed for methane–air and methanol–air flames.[1-3] The intensity of the spectra of H and O was calibrated with reference to the spectrum of O_2 with a known concentration in order to determine their absolute concentrations in the ESR cavity; while the spectral intensity of OH was calibrated with reference to the NO spectrum.[14,15] A correction for the first-order destruction of H and O on the wall of the sampling probe before reaching the ESR cavity was made by changing the residence time in the sampling probe, as described previously.[3]

A correction for the destruction of OH during sampling was rather difficult, since it did not follow a simple first-order process and was thought to be largely due to unknown reactions occurring at or close to the hole of the sampling probe.[3] The correction factor was, therefore, determined from the observed ESR intensities of H, O, OH, and O_2 in the post flame region and the assumed partial equilibrium of the reaction,

$$H + O_2 \longrightarrow O + OH, \tag{R1}$$

by using the equilibrium constant, $K=300\cdot T^{-0.372}\exp(-8565/T)$ reported previously.[16]

Stable intermediates (H_2, CH_2O, and CO) were detected together with the fuel CH_3OH and the final products (CO_2 and H_2O) by the mass spectrometric method. The concentrations of the stable species were determined from the observed intensities of their mass patterns with reference to those of the mixtures of known compositions. No correction was made for the reactions in the sampling probe for these stable species.

Figure 2 shows the concentration profiles (all in the mole fraction unit) of stable and unstable species in the flame of stoichiometric composition (CH_3OH: 11.7%, O_2: 17.7%, Ar: 70.6%) with the cold gas velocity

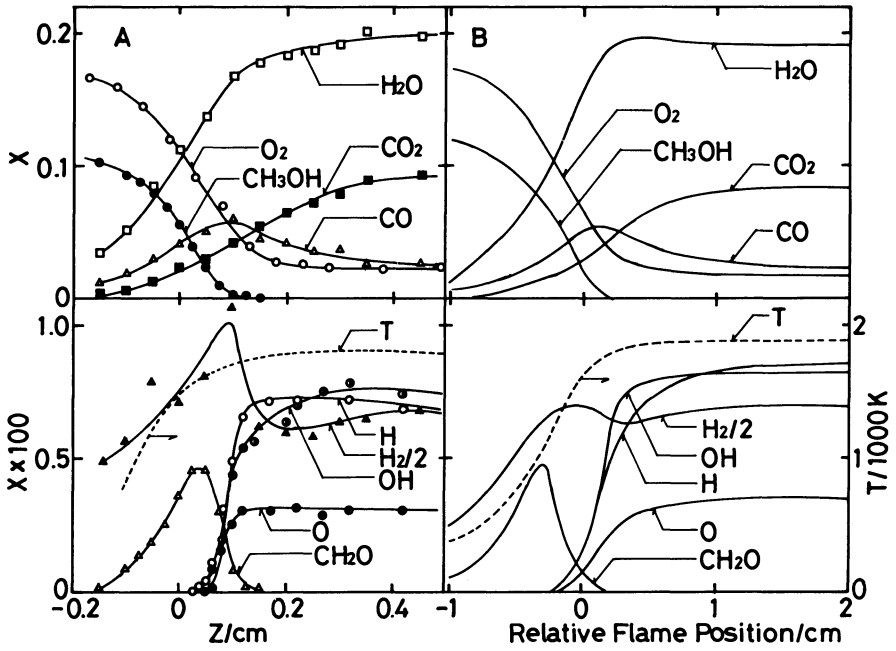

Fig. 2. The profiles of mole fractions (X) of labile and stable species and temperature (A) experimentally observed in stoichiometric methanol-oxygen-argon flame at 1.11×10^4 Pa, and (B) calculated in stoichiometric methanol-air flame at 1.01×10^4 Pa by Westbrook and Dryer (Ref. 6). The scale of abscissa is different between the observed and calculated profiles.

of 41.6 cm s^{-1} (mass flow rate of 6.36×10^{-3} g $cm^{-2}s^{-1}$). The origin of the z-axis corresponds to the beginning of the luminous zone of the flame. The observed profiles resemble those for the low-pressure methanol-air flames of the equivalence ratio (ϕ, $([fuel]/[O_2])_{actual}/([fuel]/[O_2])_{stoichiometric}$) of 1.0 observed by Andersson et al. by means of the mass spectrometric method.[4] There is a slight difference from the previous data regarding the absolute values at the concentration maximum of the profiles. This is probably due to a difference in the flame temperature. The general trend of the present concentration profiles is also very similar to that of low-pressure methanol-air flames of $\phi=1.08$.[9,10]

Westbrook and Dryer[6] have reported on the concentration profiles of chemical species in the stoichiometric methanol-air flame at 1.01×10^4 Pa which have been calculated on the basis of the numerical model of the methanol combustion including 26 species and 84 reactions. The concentration profiles observed in the present study agree with the calculated profiles (as demonstrated in Fig. 2), except that the transient change in the observed concentrations is generally steeper than that expected from model calculations. The same agreement between the observed and calculated profiles has been found for methanol-air flames at atmospheric pressure in the previous study of this series.[3] Thus, it is concluded that the numerical model proposed by Westbrook and Dryer[7] reproduces fairly well the effect of the pressure on the chemical reactions of methanol combustion. A similar conclusion has also been obtained from previous mass spectrometric studies.[4,5]

Formation and Consumption Rates of Chemical Species. In order to examine the chemical aspects of the flame more carefully, the net reaction rate, K, of each species was derived from the concentration profile and Eq. 4, and is shown in Fig. 3. The positive K value indicates net formation, while the negative value indicates net consumption.

The consumption rates of CH_3OH and O_2 and the formation rates of H_2O, H_2, and CO show maxima at almost the same positions. In contrast, the formation rate of CO_2 shows a very broad maximum at the downstream region. It is slowly formed in an extended region of the flame.

For all the labile intermediates (H, O, and OH), the K value first grows in the negative side and then changes to the positive. The features of local K values of the labile intermediates in flame indicates that the labile intermediates are supplied by backward diffusion to the upstream, preheated region, where they are effectively consumed by reactions with CH_3OH.

Reaction Mechanism. The comprehensive reaction mechanism for methanol combustion was first developed by Westbrook and Dryer[6] and was later modified.[5,8] The calculated concentration profiles for one-dimensional flames based on this reaction

mechanism have generally agreed with experimental results.[3,4,9,10] An agreement can also be seen in the present experimental results (already shown in Fig. 2).

Recently, however, Dove and Warnatz proposed a different reaction mechanism, which is simpler (14 species and 40 reactions) than the previous one and explicitly regards the pathway of methanol oxidation to be $CH_3OH \rightarrow CH_2OH \rightarrow CH_2O \rightarrow CHO \rightarrow CO \rightarrow CO_2$.[7] They have argued that the new model predicts well the experimentally observed burning velocity. The formation (or consumption) rates determined in the present experimental study will be examined with reference to the reaction mechanism proposed by Dove and Warnatz. According to the proposed mechanism,[7] CH_3OH reacts mainly with the labile intermediates (H, O, and OH) as follows:

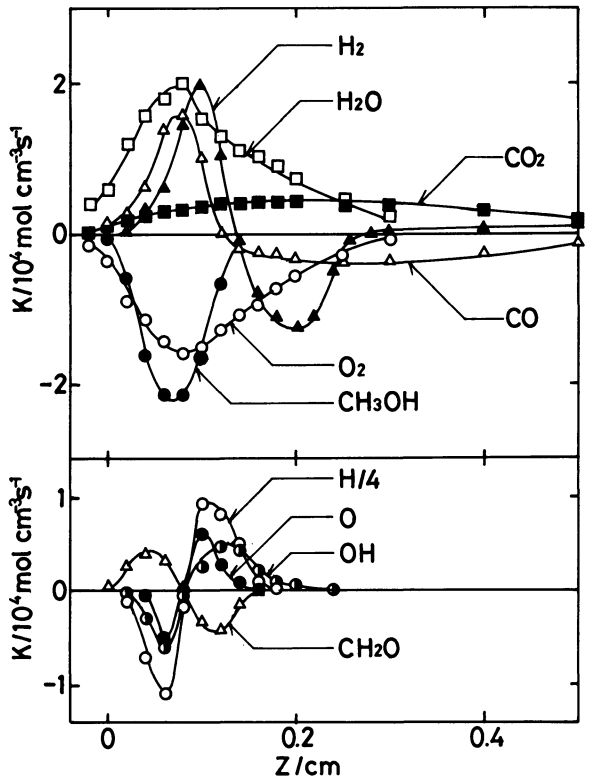

Fig. 3. Net formation (or consumption) rates of labile and stable species in the stoichiometric methanol-oxygen-argon flame at 1.11×10^4 Pa, directly derived from the observed concentration profiles in Fig. 2.

$$CH_3OH + OH \longrightarrow CH_2OH + H_2O, \quad (R2)$$
$$CH_3OH + H \longrightarrow CH_2OH + H_2, \quad (R3)$$

and

$$CH_3OH + O \longrightarrow CH_2OH + OH. \quad (R4)$$

The reactions of CH_2O, CHO, and CO are

$$CH_2O + H \longrightarrow CHO + H_2, \quad (R5)$$
$$CH_2O + O \longrightarrow CHO + OH, \quad (R6)$$
$$CH_2O + OH \longrightarrow CHO + H_2O, \quad (R7)$$
$$CHO + M \longrightarrow CO + H + M, \quad (R8)$$
$$CHO + H \longrightarrow CO + H_2, \quad (R9)$$
$$CHO + OH \longrightarrow CO + H_2O, \quad (R10)$$

and

$$CHO + O_2 \longrightarrow CO + HO_2. \quad (R11)$$

CO_2 is then formed mainly by the reaction,

$$CO + OH \longrightarrow CO_2 + H. \quad (R12)$$

Though CH_3OH can be oxidized also by HO_2 as

$$CH_3OH + HO_2 \longrightarrow CH_2OH + H_2O_2 \quad (R13)$$

and

$$CH_2O + HO_2 \longrightarrow CHO + H_2O_2, \quad (R14)$$

Table 1. Elementary Reactions of Methanol Combustion and Their Rate Parameters Used in the Discussion of the Present Experimental Results

Reaction		A	n	T_0
$H + O_2 \longrightarrow O + OH$	(R1)	2.4×10^{16}	−0.91	8310
$CH_3OH + OH \longrightarrow CH_2OH + H_2O$	(R2)	1.0×10^{13}	0	850
$CH_3OH + H \longrightarrow CH_2OH + H_2$	(R3)	4.0×10^{13}	0	3070
$CH_3OH + O \longrightarrow CH_2OH + OH$	(R4)	1.0×10^{13}	0	2370
$CH_2O + H \longrightarrow CHO + H_2$	(R5)	2.5×10^{13}	0	2010
$CH_2O + O \longrightarrow CHO + OH$	(R6)	3.5×10^{13}	0	1770
$CH_2O + OH \longrightarrow CHO + H_2O$	(R7)	3.0×10^{13}	0	600
$CO + OH \longrightarrow CO_2 + H$	(R12)	4.6×10^{6}	1.5	−370
$CO_2 + H \longrightarrow CO + OH$	(−R12)	1.6×10^{14}	0	13200
$CH_2OH + O_2 \longrightarrow CH_2O + HO_2$	(R16)	1.0×10^{13}	0	3620
$CH_2OH + M \longrightarrow CH_2O + H + M$	(R17)	1.0×10^{14}	0	12600
$CH_2OH + H \longrightarrow CH_2O + H_2$	(R18)	2.0×10^{13}	0	0

The reactions were taken from the reaction mechanism proposed by Dove and Warnatz (Ref. 7). The rate parameters are those in the expression of the reaction rate constant $k = AT^n \exp(-T_0/T)$ in cm^3 mol^{-1} s^{-1} unit.

these oxidation paths are unimportant compared with reactions R2—4 and R5—7 under the present high-temperature conditions. The rate constants of some of these reactions[7] are cited in Table 1.

The above oxidation pathway gives the formation (or consumption) rates, K, as a function of the concentrations of reacting species as following:

$$K(CH_3OH) = -\{k_{R2}[OH]+k_{R3}[H]+k_{R4}[O]\}[CH_3OH] \quad (5)$$

and

$$K(CO_2) = k_{R12}[CO][OH] - k_{-R12}[CO_2][H]. \quad (6)$$

Assuming a quasi-stationary state for CHO,

$$K(CO) + K(CO_2) = \{k_{R5}[H]+k_{R6}[O]+k_{R7}[OH]\}[CH_2O] \quad (7)$$

is also obtained. The K values can be calculated from the observed concentration profiles of the reacting species and the rate constants cited in Table 1. On the other hand, the K values have been directly observed experimentally as shown in Fig. 3 (strictly speaking, directly derived from the concentration profile of the species itself). A comparison between the observed and calculated K's will verify the relevance of the reaction mechanism on which the calculation has been made.

The calculated K is compared with the observed K for the consumption of CH_3OH (Fig. 4). Both K values agree fairly well, except that the calculated K is lower in the very upstream region. The disagreement in the upstream region is attributable to a perturbation due to the inserted sampling probe: The sampling of burning gas acts as a sink for the labile intermediates, and violates their concentration profiles determined by the balance of chemical reactions and diffusion. This effect becomes important when sampling is made at positions close to the burner mouth, since a backward diffusion of the labile intermediates (only source of the labile intermediates existing at the sampling position) is seriously hindered by the sampling probe. Such a perturbation due to the sampling probe has been experimentally shown by observing the OH concentration in the preheated zone of a propane-oxygen flame by mass spectrometric (with sampling) and UV spectroscopic (without sampling) methods.[17]

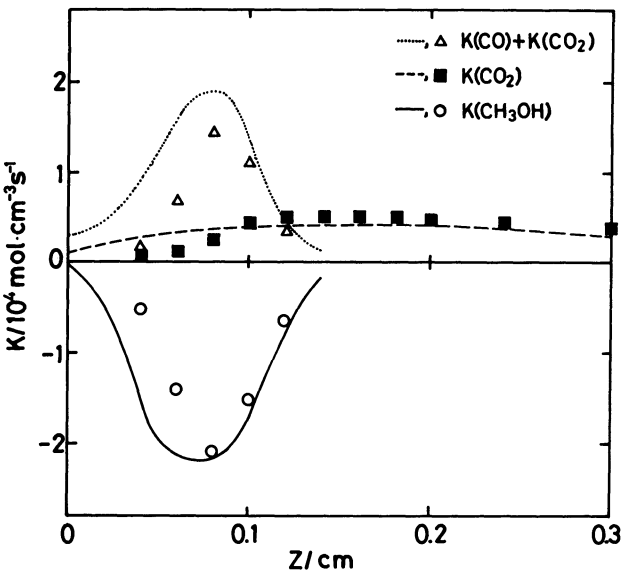

Fig. 4. Comparison between the observed (lines) and the calculated (plots) net formation (or consumption) rates of CH_3OH, CO_2, and sum of CO and CO_2. The lines showing the observed rates were taken from Fig. 3. The plots were obtained by calculating rates based on the rate constants in Table 1 and the concentration profiles of reacting species in Fig. 2. See text also for detail.

Figure 4 shows an agreement between the observation and calculation, also for $K(CO_2)$ and $K(CO)+K(CO_2)$ in the region $z>0.1$ cm, where the concentrations of the labile intermediates reach a plateau value and the perturbation due to the sampling probe is expected to be insignificant. Because the CH_2O consumption appears to balance the formation of CO and CO_2, CHO is very probably short-lived and is converted quickly to CO. Although CH_2O can react with O_2 as

$$CH_2O + O_2 \longrightarrow CHO + HO_2, \quad (R15)$$

numerical examinations based on the observed concentration profiles and the reported rate constants show that the rate of reaction R15 is much smaller than the rates of the reactions of CH_2O with H, O, and OH (reactions R5—7) throughout the flame.

The general agreement between the observed and calculated K values indicates a consistency between the observed concentration profiles of labile and stable chemical species in the flame, and gives experimental support to the simpler mechanism of methanol oxidation.

According to the Dove and Warnatz's mechanism,[7] the consumption of O_2 is mostly due to the following reactions:

$$H + O_2 \longrightarrow O + OH \quad (R1)$$

and

$$CH_2OH + O_2 \longrightarrow CH_2O + HO_2. \quad (R16)$$

The rate of O_2 consumption is, therefore, given as

$$-K(O_2) = \{k_{R1}[H] + k_{R16}[CH_2OH]\}[O_2] - k_{-R1}[O][OH]. \quad (8)$$

However, the consumption rate cannot be calculated in a straight-forwatd manner from the observed concentration profiles, since no experimental data is available for the CH_2OH concentration. If one

assumes that the decay of CH_2OH is exclusively due to its oxidation into CH_2O by

$$CH_2OH + O_2 \longrightarrow CH_2O + HO_2, \quad (R16)$$
$$CH_2OH + M \longrightarrow CH_2O + H + M, \quad (R17)$$

and

$$CH_2OH + H \longrightarrow CH_2O + H_2, \quad (R18)$$

reactions of CH_2OH will determine the sum of the formation rates:

$$K(CH_2O) + K(CO) + K(CO_2) = \{k_{R16}[O_2] + k_{R17}[M] + k_{R18}[H]\}[CH_2OH]. \quad (9)$$

Substituting $[CH_2OH]$ of equation 9 into equation 8,

$$-K(O_2) = k_{R1}[H][O_2] - k_{-R1}[O][OH] + k_{R16}[O_2]\frac{K(CH_2O)+K(CO)+K(CO_2)}{k_{R16}[O_2]+k_{R17}[M]+k_{R18}[H]}. \quad (10)$$

Thus, the O_2 consumption rate can be calculated from the observed $K(CH_2O)$, $K(CO)$, $K(CO_2)$, $[O_2]$, [M], and [H] and from the rate constants cited in Table 1 (the rate constant k_{-R1} can be obtained from the k_{R1} value and the equilibrium constant for reaction R1).

The calculated $-K(O_2)$, by using the rate constants in Table 1, is shown in Fig. 5 (curve B). Thus, calculated $-K(O_2)$ differs from the $-K(O_2)$ determined directly from the observed concentration profile of O_2 (curve A), especially in the downstream region. The agreement between the calculated and observed $-K(O_2)$ is much improved in the downstream region (curve C in Fig. 5), if one uses the rate constant, $k_{R1}=1.2\times10^{17}T^{-0.91}\exp(-8310/T)$, recently recommended by Warnatz.[18] This is five times as large as the previous rate constant (cited in Table 1) at the present flame temperature.

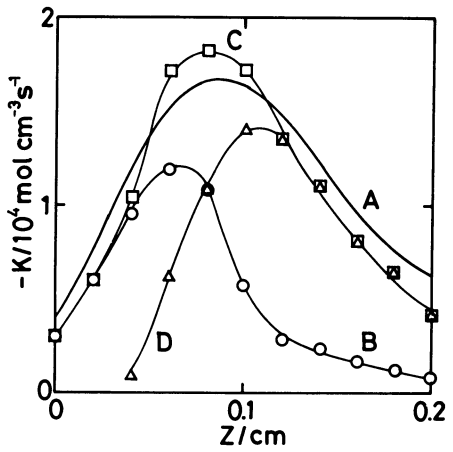

Fig. 5. Comparison of the consumption rates of O_2 obtained in different ways. (A): The observed rate taken from Fig. 3. (B): The rate calculated based on equation 10 and by using the rate constants in Table 1. (C): The rate calculated by using the newly-recommended rate constant for reaction R1. (D): The rate calculated with the newly-recommended rate constant and by excluding reaction R16. See also the text for detail.

$K(O_2)$ calculated with the new K_{R1} and neglecting reaction R16 is also shown in Fig. 5 (curve D). It is evident that reaction R16 is an important process for O_2 consumption in the upstream region of the flame. The observed $-K(O_2)$ appears to agree well with the calculation including reaction R16 rather than the calculation excluding it. We do not, however, dare to stress this agreement in the upstream region, since there is some ambiguities related to perturbation due to the inserted sampling probe in this region (as mentioned before).

Concluding Remarks. Together with seven stable species, three labile intermediates were observed in the CH_3OH-Ar-O_2 stoichiomeric flame at a low pressure by the combined ESR-mass spectrometric method. Their concentration profiles and the local distribution of their net formation (or consumption) rates in the flame were examined to elucidate the chemical reactions of methanol combustion.

The experimental results agree with the concentration profiles predicted by numerical calculations based on the model for methanol combustion consisting of very many elementary reactions previously reported by Westbrook and Dryer.[6] However, the results are also shown to be consistent even with the simplified model for the methanol combustion recently proposed by Dove and Warnatz.[7] As far as the authors are aware, the present study provides some of the most comprehensive experimental data on the distribution of the chemical species in a methanol flame. There is still no need to make the reaction mechanism complex in order to interpret the present experimental results. This does not necessarily means that the reaction mechanism of methanol combustion is really simple. Further progress in combustion chemical experiments is desirable for unambiguous comparisons with the proposed models and to totally elucidate the chemical aspect of combustion.

References

1) S. Noda, M. Miura, and H. Yoshida, *J. Phys. Chem.*, **84**, 3143 (1980).

2) S. Noda, H. Demise, O. Claesson, and H. Yoshida, *J. Phys. Chem.*, **88**, 2552 (1984).

3) M. Taniguchi and H. Yoshida, *Bull. Chem. Soc. Jpn.*, **60**, 1249 (1987), the preceding paper of this series).

4) L. L. Andersson, B. Christenson, A. Höglund, J. O. Olsson, and L. G. Rosengren, *Prog. Astronaut. Aeronaut.*, **95**, 164 (1984).

5) J. O. Olsson, L. S. Karlsson, and L. L. Andersson, *J. Phys. Chem.*, **90**, 1458 (1986).

6) C. K. Westbrook and F. L. Dryer, *Combust. Flame*, **37**, 171 (1980).
7) J. E. Dove and J. Warnatz, *Ber. Bunsenges. Phys. Chem.*, **87**, 1040 (1983).
8) C. K. Westbrook, F. L. Dryer, and K. P. Schug, *Symp. (Int.) Combust. [Proc.]*, **19**, 153 (1982).
9) R. Akrich, C. Vovelle, and R. Delbourgo, *Combust. Flame*, **32**, 171 (1978).
10) J.-F. Pauwels, M. Carlier, and L.-R. Sochet *J. Phys. Chem.*, **86**, 4330 (1982).
11) J. Vandooren and P. J. Van Tiggelen, *Symp. (Int.) Combust. [Proc.]*, **18**, 473 (1981).
12) A. A. Westenberg and R. M. Fristrom, "Flame Structure," McGraw Hill, New York (1965), p. 276.
13) J. Warnatz, *Symp. (Int.) Combust. [Proc.]*, **18**, 369 (1981).
14) A. A. Westenberg and N. de Haas, *J. Chem. Phys.*, **40**, 3087 (1964).
15) A. A. Westenberg, *J. Chem. Phys.*, **43**, 1544 (1965).
16) G. Dixon-Lewis and D. J. Williams, "Comprehensive Chemical Kinetics," ed by C. H. Bamford and C. F. H. Tipper, Elsevier, Amsterdam (1977), Vol. 17, p. 91.
17) J. M. Revet, D. Puechberty, and M. J. Cottereau, *Combust. Flame*, **33**, 5 (1978).
18) J. Warnatz, "Combustion Chemistry," ed by W. C. Gardiner, Jr., Springer, New York (1984), Chap. 5.